Functionalization of graphene nanostructures with inorganic nanoparticles and their use for the removal of pharmaceutical pollutants in water

Jana Oliveras, Lionel Marcon, Neus G Bastús, Victor Puntes

Functionalization of Graphene Nanostructures with Inorganic Nanoparticles and Their Use for the Removal of Pharmaceutical Pollutants in Water

Jana Oliveras, Lionel Marcon, Neus Bastus, Victor Puntes

Functionalization of Graphene Nanostructures with Inorganic Nanoparticles and Their Use for the Removal of Pharmaceutical Pollutants in Water

Victor Puntes[1, 2*], Jana Oliveras[2], Lionel Marcon[3], Neus Bastus[2*]

[1]Vall d'Hebron Research Institute (VHIR), Spain, [2]Institut catala de Nanociencia i Nanotecnologia, Spain, [3]UMR5306 Institut Lumière Matière (ILM), France

Submitted to Journal:
Frontiers in Chemical Engineering

Specialty Section:
Environmental Chemical Engineering

Article type:
Original Research Article

Manuscript ID:
1084035

Received on:
29 Oct 2022

Revised on:
04 Dec 2022

Journal website link:
www.frontiersin.org

Conflict of interest statement

The authors declare that the research was conducted in the absence of any commercial or financial relationships that could be construed as a potential conflict of interest

Author contribution statement

Jana Oliveras and Lionel Marcon performed the absorption experiments, Jana Oliveras and Neus bastus performed the NP synthesis and characterization, Lionel Marcon, Neus Bastus and Victor Puntes designed the experiments and Neus Bastus and Victor Puntes wrote the manuscript.

Keywords

Graphene, nanomagnetite, photocatalysis, remediation, pharmaceuticals

Abstract

Word count: 143

A graphene-based hybrid material decorated with Fe3O4 and TiO2 nanoparticles (NPs) to effectively remove emerging pollutants as non-steroidal anti-inflammatory drugs (NSAIDs) Ibuprofen and Diclofenac present in water at low environmental concentrations has been prepared by a one-step functionalization process following a novel gentle and scalable surfactant-depletion approach. Following this method, NPs are progressively deprived of their original surfactant in the presence of graphene, leading to the formation of hybrid nanostructures composed of two different types of NPs well dispersed over the graphene nanosheets. The as-prepared hybrid material possesses high adsorption capacity, superparamagnetic properties, photocatalytic behaviour, and good water dispersibility. Ibuprofen and Diclofenac adsorption kinetics on the composites was investigated via UV-Vis spectroscopy. Thanks to incorporating TiO2 NPs as in situ catalysts, the adsorption performance of composites is restored after use, which could be a promising recycling pathway for the adsorbents in wastewater treatments.

Contribution to the field

We present a straight forward method for decorating graphene and graphene oxide with inorganic nanoparticles for the capture and degradation of organic pollutants. The hybrids are employed to remove ibuprofen and diclophenac from water, serious pollutants producing evere damage at low concentrations

Ethics statements

Studies involving animal subjects

Generated Statement: No animal studies are presented in this manuscript.

Studies involving human subjects

Generated Statement: No human studies are presented in this manuscript.

Inclusion of identifiable human data

Generated Statement: No potentially identifiable human images or data is presented in this study.

Data availability statement

Generated Statement: The original contributions presented in the study are included in the article/supplementary material, further inquiries can be directed to the corresponding author/s.

Functionalization of Graphene Nanostructures with Inorganic Nanoparticles and Their Use for the Removal of Pharmaceutical Pollutants in Water

Jana Oliveras[1], Lionel Marcon[2], Neus G. Bastús [1*] and Victor Puntes[1, 3,4*]

[1] Institut Català de Nanociència i Nanotecnologia (ICN2), CSIC, The Barcelona Institute of Science and Technology (BIST), Campus UAB, Bellaterra, Barcelona, Spain.
[2]Institut Lumière Matière, UMR CNRS 5306, UCBL, Campus LyonTech - La Doua, Bâtiment Raulin, 10 rue Ada Byron, 69622 Villeurbanne, France
3 Institució Catalana de Recerca i Estudis Avançats (ICREA), 08010 Barcelona, Spain.
4 Vall d'Hebron Institut de Recerca (VHIR), 08035, Barcelona, Spain.
+CIBER

*neus.bastus@icn2.cat, victor.puntes@icn2.cat

ABSTRACT

A graphene-based hybrid material decorated with Fe_3O_4 and TiO_2 nanoparticles (NPs) to effectively remove emerging pollutants as non-steroidal anti-inflammatory drugs (NSAIDs) Ibuprofen and Diclofenac present in water at low environmental concentrations has been prepared by a one-step functionalization process following a novel gentle and scalable surfactant-depletion approach. Following this method, NPs are progressively deprived of their original surfactant in the presence of graphene, leading to the formation of hybrid nanostructures composed of two different types of NPs well dispersed over the graphene nanosheets. The as-prepared hybrid material possesses high adsorption capacity, superparamagnetic properties, photocatalytic behaviour, and good water dispersibility. Ibuprofen and Diclofenac adsorption kinetics on the composites was investigated via UV-Vis spectroscopy. Thanks to incorporating TiO_2 NPs as *in situ* catalysts, the adsorption performance of composites is restored after use, which could be a promising recycling pathway for the adsorbents in wastewater treatments.

INTRODUCTION

Nanoremediation refers to the use of nanostructures for efficiently capturing and degrading pollutants in water and soils, being a new solution to address the challenge of cleaning and making water drinkable in a simple, affordable, and scalable manner[1].

Emerging pollutants, especially pharmaceutically active compounds, have become a concern when present in the environment despite their low concentration[2-5]. These compounds are inherently designed to interact with biological systems. They are usually excreted -to some extent- non-metabolized by humans and livestock[6], directly to wastewater or in sludge, later used as fertilizer.[7,8] Up to now, over 200 pharmaceutical products have been detected in freshwaters; the most commonly found are antibiotics, followed by painkillers, analgesics and antidepressants.[9]

Within these pharmaceutically active compounds, non-steroidal anti-inflammatory drugs (NSAIDs) are of significant concern as highly persistent pollutants, threatening the well-being of living species.[10] These compounds display a heightened ability to diffuse passively across biological membranes and increased persistence in aquatic environments[11]. Although environmental concentrations are relatively low -µg/L to g/L in seawaters[12], and ng/L in ground and drinking waters[13]-. They can be transported to other compartments (e.g., air, soil), concentrate and metabolize into equally or even more toxic substances[14-16]. Ibuprofen (IBP) and Diclofenac (DCF) are especially critical among NSAIDs.[10] They are estimated to be consumed in several kilotons per year globally, and their consumption tends to increase, accompanied by wide usage and irresponsible disposal.

Although significant advances have been made, conventional treatment methods are still incapable enough of treating the persistency of these compounds[17-19]. Thus, despite reducing the concentration of these pharmaceuticals, a necessity of posttreatment to remove them is needed[20]. Adsorption appears to be the most broadly feasible removal method because of its versatility, broad applicability and economic feasibility. Numerous adsorbents have been developed, such as activated carbon, nanocomposites, metal frameworks and polymeric porous materials. [21-22] However, they have the disadvantage of low adsorption capacity, difficult separation from water, and challenging reuse after adsorption. Alternatively, advanced oxidation processes (AOP) offer great potential to degrade and mineralize NSAIDs.[23-26] However, they often produce metabolites that are more problematic than the initial compound. Therefore, developing a cost-efficient removal technique for NSAIDs from aqueous media with a high adsorption capacity, facile separation and easy regenerability is still not fully developed.

"Graphene and graphene oxide-based materials (GMs) have been considered promising adsorbents for environmental decontamination due to their high surface area (~2630 $m^2 g^{-1}$), large delocalized pi (π) electrons, and tunable chemical properties [26-29]. However, GMs in solution pose an additional pollution risk because they cannot be fully separated due to their nanoscale dimensions [31] dimensions[10]Additionally, their functionalization with inorganic nanoparticles (NPs) exhibits other

advantageous and often synergistic behaviour.[30] For example, adding magnetic NPs to graphitic structures allows for quickly removing the adsorbent materials from the treated waters[31-32] while the semiconductor NPs adsorbed in the GMs could provide new ways to degrade photocatalytically NSAIDs efficiently[33-34]. However, despite the great potential of GMs, there are few papers currently published in the literature reporting on the use of GMs for the removal of IBP and DCF, mainly graphene oxide and reduced graphene-oxid, and showing indeed a relatively low adsorption capacity[35-38]. Additionally, none includes the functionalization of the GMs with inorganic NPs. Therefore, developing graphene-based hybrid materials for NSAIDs adsorption requires new studies on this topic.

Functionalization of GMs with magnetic Fe_3O_4 NPs are based on *in situ* and *ex situ* strategies. A straightforward approach includes the growth of Fe_3O_4 NPs directly on the surface of GMs following chemical treatments, heating or electrodeposition of precursors electrostatically absorbed at the surface of GMs.[28, 42-45] Alternatively, GM-Fe_3O_4 hybrid composites can be produced by *ex situ* assembly. In this process, Fe_3O_4 NPs are synthesized in advance and subsequently attached to the surface of GM via electrostatic or covalent interactions.[46-48] Both approaches present appealing benefits but also significant limitations. While the direct formation of the NPs onto GMs is simple, and large amounts of Fe_3O_4 NPs can be immobilized, uncontrollable reactions over the GM surface lead to limited control of NPs morphology (size, shape). On the other hand, the attachment of pre-formed NPs to GM is a more complex procedure that typically involves chemical modifications of both components and interconnection. Although it allows for NP morphological control and finer loading adjustment, it may require tedious and complicated surface modification processes. Remarkably, neither of the synthetic approaches provides a straightforward production of Graphene–NP hybrid structures composed of different types of NPs.

In this work, we designed a novel graphene-based hybrid material decorated with Fe_3O_4 and TiO_2 NPs to effectively remove IBP and DCF present at environmental concentrations. The adsorption kinetics of IBP and DCP by GM hybrid nanostructures, whose rates depend much on the type of compound analyzed, its concentration, and the adsorbent used, were investigated via UV-Vis spectroscopy.[49] Note that water purification at low pollutant concentrations is often more challenging than at higher concentrations, where physical and chemical approaches can be efficiently applied if the water is not significantly polluted and still holds some life.[50]

The novelty of this work relies on two distinct aspects. First, the materials' preparation presents remarkable advantages concerning state-of-the-art functionalization strategies. Herein, easily scalable one-step reaction (slow reaction at room T, therefore no critical mass or temperature gradients during synthesis). following a novel surfactant-depletion approach similar to the one developed for CNTs functionalization [51]. Following this method, NPs are slowly deprived of their original surfactant layer in the presence of graphene, leading to the formation of hybrid nanostructures composed of different types of NPs well dispersed over the graphene nanosheets while avoiding NP-NP aggregation. The

second novel aspect relies on the additivity of the obtained structures. Thus, beyond showing a high adsorption capacity and good water dispersibility, hybrid structures are also superparamagnetic at room temperature, which allows their quickly removed by using a magnet, and thanks to incorporating TiO2 NPs, they are photocatalysts, so the absorbed material can be degraded and the adsorption performance partially restored, which seems a promising regeneration strategy.

RESULTS AND DISCUSSION

Rational of Functionalization of GM with Inorganic Nanoparticles

The functionalization of graphene with inorganic NPs is based on the controlled destabilization of the NPs from their original surfactant layer, which typically provides stability. Under the appropriate conditions, the original surfactant layer of the NP is depleted in a controlled manner, while graphene act as a "surrogate ligand", trapping the partially surfactant-depleted NPs, leading to 2D hybrid structures selectively decorated with NPs of controlled physicochemical features. This is achieved when low-binding surfactant stabilizers are employed. In these cases, there is a need for free surfactant in solution in equilibrium with the surfactant at the NP surface. So that if the free surfactant is removed, the NP surface is progressively stripped.

At short times, the direct exposition of as-synthesized NPs to GM does not result in the functionalization of the graphene structure. As time goes by and the surfactant is removed from the surface, NPs, are still stable against NP-NP aggregation but able to interact with the GM, resulting in GM decoration. On the contrary, fast depletion of the surfactant would lead to NPs aggregation in the solution prior to the adsorption onto the graphene in an aggregated form (**Scheme 1**). To control these conditions, the surfactant at the NP has to be in dynamic equilibrium with an excess of surfactant in the solution and then place the graphene-NP mix in a dialysis bag to promote slow surfactant depletion. The presented method is RT, straightforward, versatile, highly reproducible, recyclable, and scalable, thereby representing an exciting approach for the modular development of inorganic carbon-supported hybrid structures.

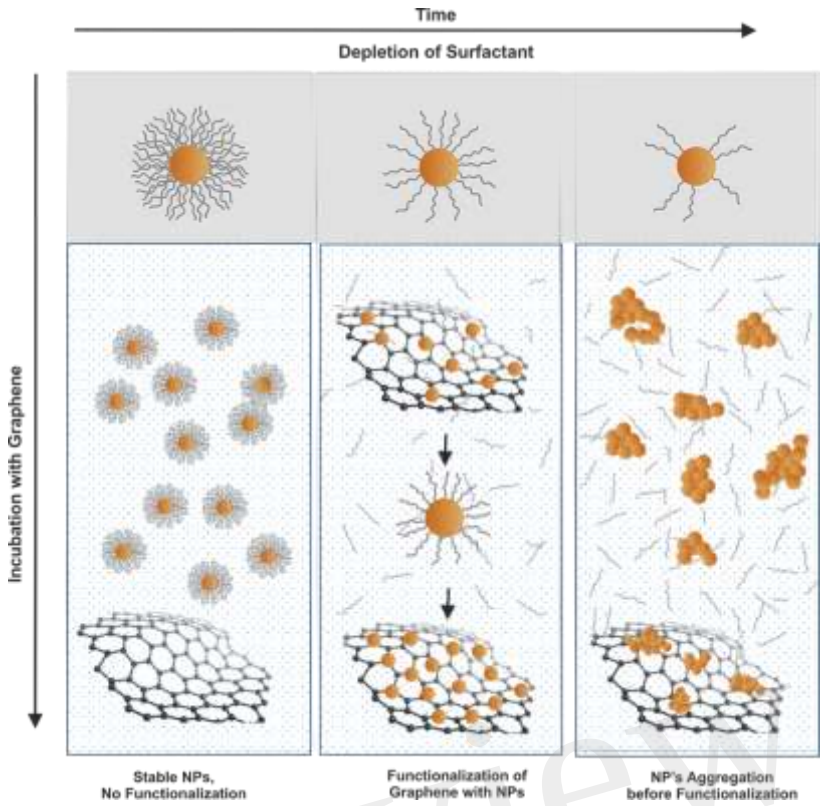

Scheme 1. Functionalization process of graphene with inorganic nanoparticles. The surfactant at NP's surface is depleted by dialysis in the aqueous media in which the graphene is solubilized. The complete depletion of the surfactant leads to NP's aggregation before its attachment to graphene, while the direct exposition of as-synthesized NPs to Graphene does not allow the functionalization of the graphene structure. In between, the control of the process enables the selective functionalization of graphene with inorganic nanoparticles.

Synthesis and characterization of graphene oxide/Fe3O4/TiO2 hybrid nanostructures

Graphene (G, purity >99%, layers <3) was used as received without further purification. Highly monodisperse magnetite ~7 nm Fe_3O_4 NPs (1mg NPs/mL) and ~7.5 nm TiO_2 NPs (1mg NPs/mL) chemically stabilized with tetramethylammonium hydroxide (TMAOH) as surfactant were prepared following well-established synthetic procedures[52-53]. Representative transmission electron microscopy

(TEM) images of as-obtained Fe_3O_4 NPs and TiO_2 NPs (

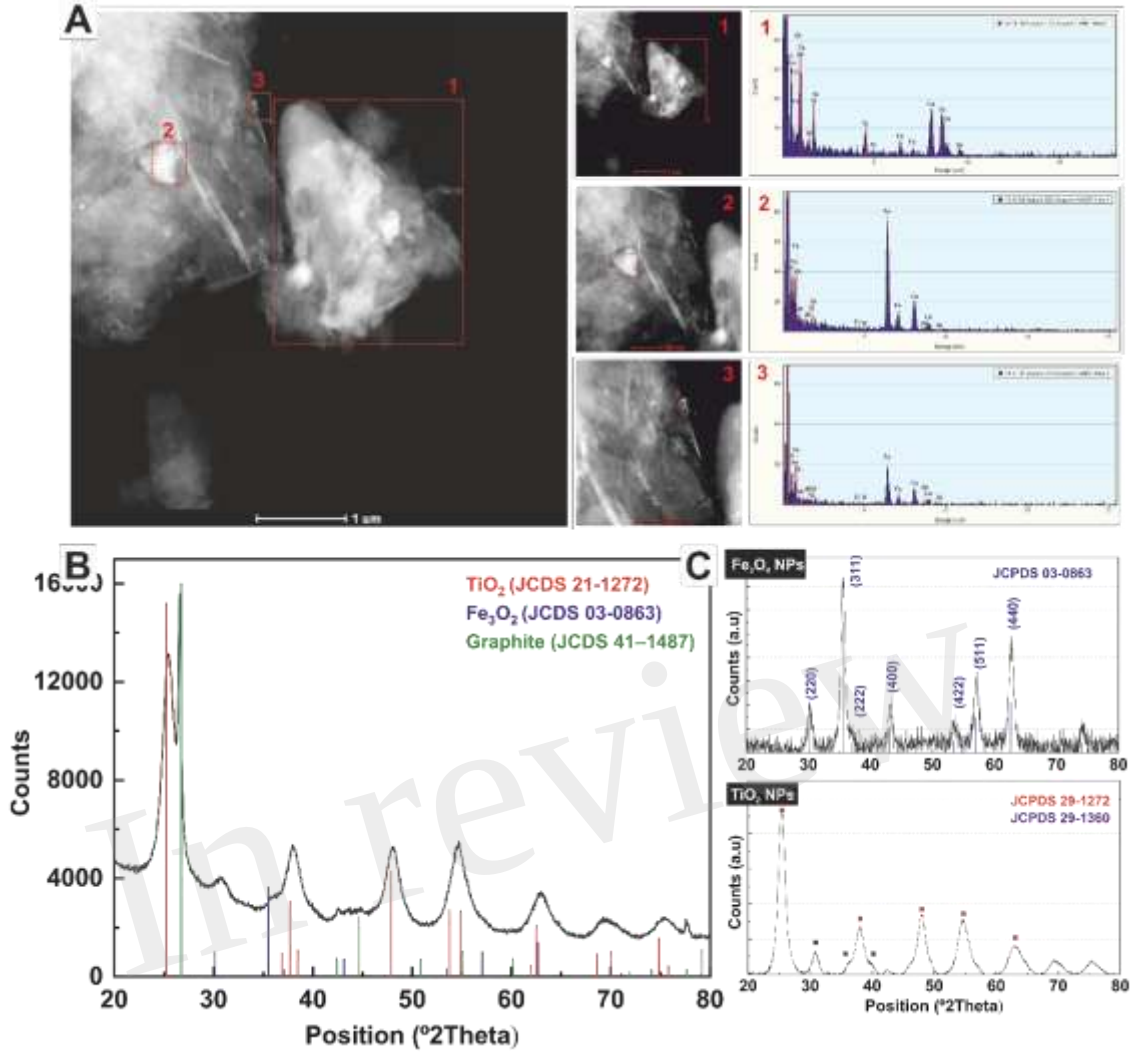

Figure 2. A) EDS analysis of the Graphene/ Fe3O4/TiO_2 hybrids structures. Scan profiles extracted from the representative sections of the HAADF-STEM images (as labelled) confirmed the presence of both types of NPs at the surface of the graphene sheet. The Cu peaks are the signal detected from the TEM grid. B) XRD of Graphene/ Fe_3O_4/TiO_2 structures. C) XRD of Fe_3O_4 and TiO_2 NPs.

A) reveal the formation of highly uniform particles with well-defined morphologies. Structural characterization by X-ray diffraction (**Fig. S1**) shows well-defined peaks accordingly to the high crystallinity of the sample.

GM/Fe_3O_4/TiO_2 hybrid nanostructures were prepared by adding a known volume of Fe_3O_4 NPs (16 µL, 1 mg/mL, 3.2 10^{12} Fe_3O_4 NPs/1mg graphene) to 1 mL of an aqueous solution of graphene (5 mg/mL) and left stirring for 3 days in a dialysis bag (6 cycles) against 5 litres of H_2O. This process causes osmotic stress, which leads to the slow and progressive surface depletion of surfactant from the NP surface towards the counter-dialyzing solution. This process typically results in NP aggregation. However, adding the GM to the system results in the functionalization of the graphene sheets with NPs in a randomly distributed manner (**Fig. 1 and S2**). Once the NP is absorbed into the GM, the surfactant

completely abandons the NP surface yielding NPs with a clean surface that directly attaches to the graphene, as observed by high-resolution TEM **(Fig.S3).** The resulting hybrids were purified, and a controlled volume of TiO_2 NPs ($3.2\ 10^{12}$ TiO_2 NPs/1mg graphene) was added to the aqueous graphene/Fe_3O_4 solution. Then, the above-described incubation process was repeated, yielding GM/Fe_3O_4/TiO_2 hybrid nanostructures. The robustness of the graphene hybrid final product was tested by ultra-sonication for up to 30 min without any observable change in morphology or NP detachment.

The morphology and structure of representative hybrids were investigated by scanning electron microscopy (SEM), high-angle annular dark-field scanning TEM (HAADF-STEM) and High-Resolution TEM (HR-TEM). SEM images reveal that NPs are uniformly attached on graphene sheets, which correlates with the bright spots in the HAADF-STEM images (**Fig. 1B**). As is evident in the HR-TEM (**Fig 1C)**, graphene is highly electron transparent, and the contrast here is due to three or more graphene layers. Results suggest that NPs are directly linked to the sheet, with no distance between the NPs and the graphene (**Fig. 1C**).

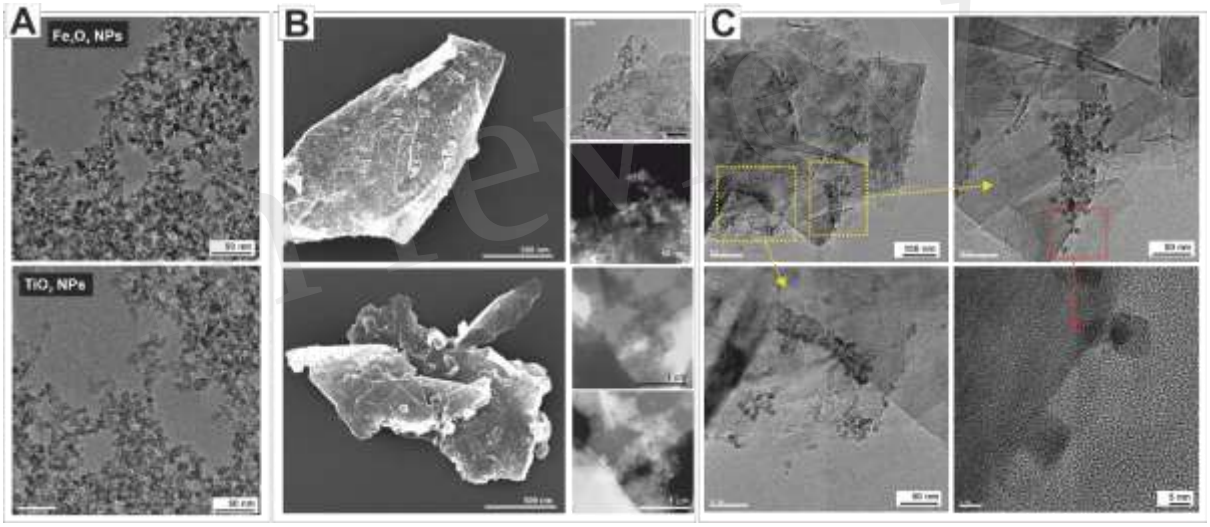

Figure 1. Representative Electron Microscopy Images of NPs and NPs/Graphene hybrids structures. A) Transmission electron microscopy (TEM) images of as-synthetized Fe_3O_4 and TiO_2 NPs TEM. B) Scanning Electron Microscopy (SEM), TEM and Scanning Transmission Electron Microscopy (STEM) taken with a high-angle annular dark field (HAADF) detector of GM/Fe_3O_4/TiO_2 hybrid nanostructures. C) High-Resolution TEM (HRTEM) images of GM/Fe_3O_4/TiO_2.

The similar size and morphology of Fe_3O_4 NPs (~7 nm) and TiO_2 (~7.5 nm) make their discrimination difficult. Thus, the chemical composition analysis of the structure was assessed by Energy Dispersive X-Rays Spectroscopy (EDS) analysis (**Fig. 2A, Fig. S4**), where scan profiles extracted from the representative sections of the HAADF-STEM images confirmed the presence of both types of NPs at the surface of the graphene sheet. In addition, the crystallographic structures of the graphene hybrid nanostructures were also studied by XRD analysis (**Fig. 2B**). The characteristic diffraction peak of graphite at 26º (JCPDS Card no. 41-1487) corresponding to the interplanar distance between graphene

sheets (d = 0.345 nm) confirms that graphene substrate remained unaltered after the functionalization process. Furthermore, the most intense anatase TiO_2 peaks (JCPDS Card no. 21-1272) found at 24.8º, 37.3º, 47.6º, 53.5º, 55.1º and 62.2º correspond to (101), (004), (200), (105), (211) and (204) crystal planes are similar to that of the free TiO_2 NPs. The diffraction spectrum also reveals the presence of Fe_3O_4 NPs. XRD patterns of the Fe_3O_4 and TiO_2 NPs and corresponding standard diffraction peaks of Fe_3O_4 (JCPDS card No. 03-0863) and TiO_2 (No. 29-1272 -anatase- and No. 29-1360 -brookite) are shown in **Fig.2C**. However, the iron fluorescence irradiated with X-ray from copper makes a much weaker signal, always hidden in the background of TiO_2 NPs, no matter how long is the acquisition time. In any case, the presence of significant Fe_3O_4 NPs can be observed in the magnetic response of the solution (**Fig 3**).

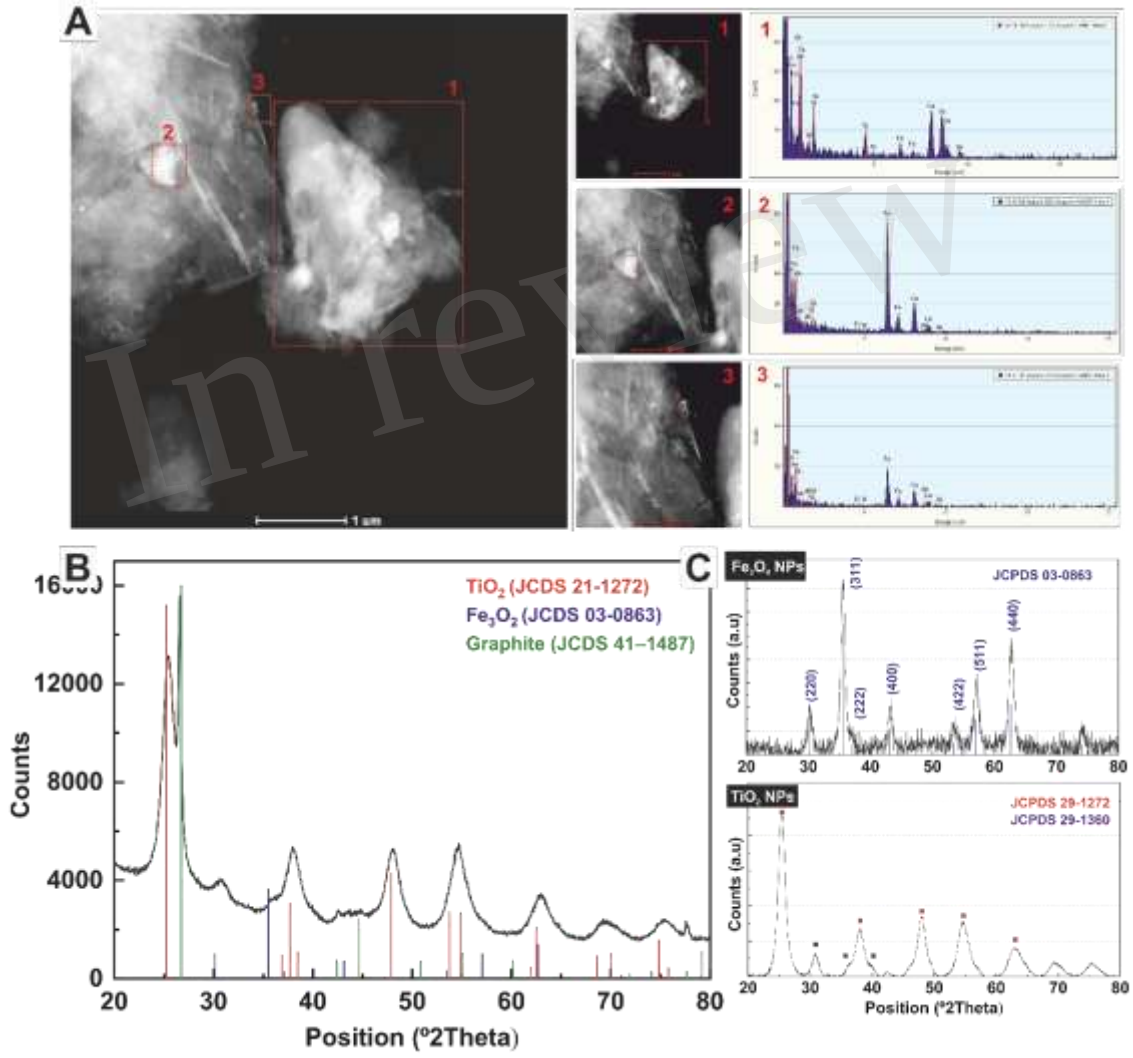

Figure 2. A) EDS analysis of the Graphene/ Fe3O4/TiO_2 hybrids structures. Scan profiles extracted from the representative sections of the HAADF-STEM images (as labelled) confirmed the presence of both types of NPs at the surface of the graphene sheet. The Cu peaks are the signal detected from the TEM grid. B) XRD of Graphene/ Fe_3O_4/TiO_2 structures. C) XRD of Fe_3O_4 and TiO_2 NPs.

The two essential goals of this procedure are the magnetic and photocatalytic modification of the graphene sheet and the aqueous solubility of the final products. Figure 3 shows the solution response to a permanent magnet and its magnetic cleaning. The magnetic characteristics of the hybrid was assessed at 10 K and 300K. While a small hysteresis is observed at low T, at RT, a canonical superparamagnetic behaviour with no hysteresis is observed, with a magnetic remanence of 0.5 the saturation magnetization, suggesting that NPs are well dispersed and non-aggregated. Interestingly, the magnetic properties are similar despite their absorption to the GM, indicating that the NPs have been individually added to the GM and not as aggregates. Otherwise, an increase in remanence and hysteresis would appear due to interparticle dipolar interactions. Using as a reference the magnetic saturation value reported in the literature[54], the weight percentage of Fe_3O_4 NPs was calculated to be around 4%, by which agrees with the measurements extracted from thermogravimetry analysis (**Fig. S5).**

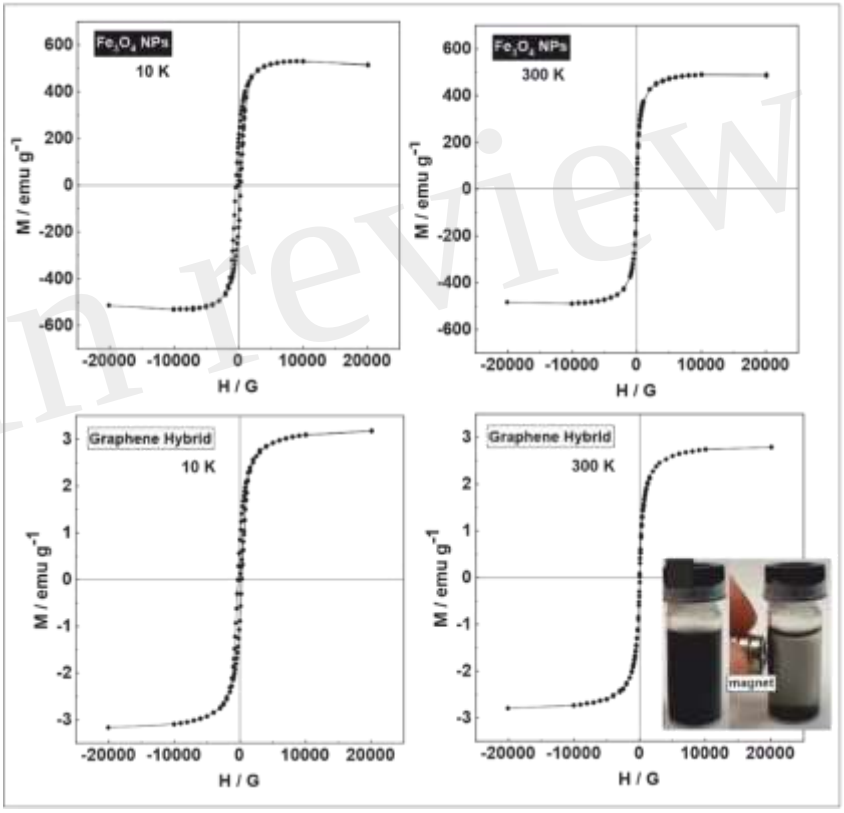

Figure 3. Magnetic behaviour of the graphene hybrid nanostructures dispersed in H_2O and its response to a permanent magnet. SQUID hysteresis loops from Fe_3O_4 NPs and graphene hybrids structures. Optical picture of distinctive coloured solutions from composite dispersed in H_2O and its response to a permanent magnet. (Inset)

Adsorption experiments

Several drug absorption experiments have been performed, exposing both graphene hybrids and plain graphene as a control for further comparison. It is generally accepted that the adsorption process on GMs involves the combination of electrostatic and non-electrostatic interactions, including π–π

electron donor-acceptor interactions and hydrophobic and electrostatic interactions [38, 55]. IBP solutions were prepared in pH ~6.3 Phosphate Buffer Solution (PBS) for optimal dissolution of the compound[52], while DCF was dissolved directly in Milli-Q water. UV-Vis was employed to analyze drug concentration after the proper calibrations (**Fig. 4**). IBP signal was observed at the characteristic band at 222nm[54] (**Fig. 4A**), and DCF signal was monitored at 275nm[53] (**Fig. 4B**). The experiments were carried out in triplicate. The adsorption process has been observed mainly to occur in the first 80 min of exposure (**Fig.4C**). Samples were left for at least 2 h to ensure complete adsorption. Then, samples were purified magnetically to separate adsorbed from the non-adsorbed drug, and the supernatant was analyzed by UV-Vis spectroscopy. Purification by centrifugation yielded similar results, indicating that all graphene has been decorated with NPs.

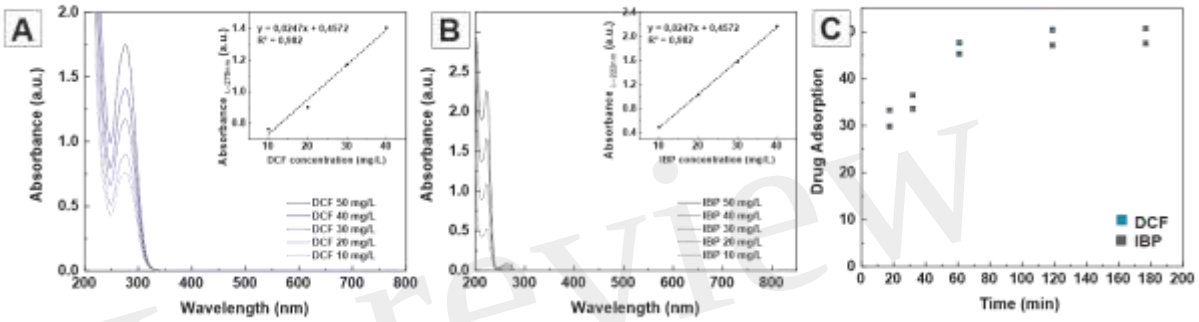

Figure 4. Calibration curves of IBP (A) and DFC (B) compounds. Time evolution experiment of Graphene Hybrids when exposed to different drugs (C). Aliquots containing 1g/L ($3.2 \cdot 10^{15}$ NPs/g graphene) Graphene hybrids were exposed to 100 mg/L and 68 mg/L for IBP and DCF solutions for different times. Adsorption was calculated from the abatement of the UV-Vis signal of the supernatant resulting from centrifuging the samples at 10000g for 10 minutes. DCF signal was monitored at 275nm, while IBP signal was observed at the characteristic band at 222nm and its temporary products at 264nm.

In the first round of experiments, the drug concentration was set constant at the reported EC_{50} -half of the drug concentration at which its maximum acute toxicity is observed- for sentinel aquatic species (*Daphnia Magna*), considered a standard in regulatory toxicology.[14, 56] These values are 100 mg/L for IBP and 68 mg/L for DCF in water, respectively. Graphene concentration was varied from 0.01 to 1 g/L. All final concentrations (**Table S1**). In a second round, the concentration of graphene sheets was constant, while drug concentration varied from 10-100 mg/L for IBP or 1-68 mg/L for DCF (**Table S2**).

Adsorption experiments revealed a consistent dose-response behaviour (**Fig. 5**). When the graphene hybrid concentration was fixed at 1g/L ($3.2 \cdot 10^{15}$ NPs/g graphene), almost the complete removal of 10 mg/L of IBP (**Fig. 5A**, in grey) or DCF (**Fig. 5B**, in blue) was achieved. On the other hand, when the drug concentration was maintained at 100mg/L IBP or 68mg/L DCF, hybrids showed increased drug adsorption for increased concentrations of hybrids, as expected (**Fig. 5C-D**). In both cases, the maximum adsorption capacity of the hybrid at the highest drug concentration tested is about 50%.

Bare graphene exposed to the drugs (**Fig. 5,** striped patterns) showed slightly better adsorption rates than the hybrid counterparts, especially at high concentrations of drug and graphene. This fact could be attributed to the presence of NPs that block the adsorption sites of the graphene. To test this hypothesis, we studied the impact of NPs density on the drug adsorption by preparing graphene hybrids with different NP concentrations (0, $3.2 \cdot 10^{14}$, $3.2 \cdot 10^{15}$, $3.2 \cdot 10^{16}$ NPs/g graphene; Graphene] = 1 g/L) and exposing them to 68 mg/L and 100 mg/L for DCF and IBP respectively solutions (see **Table S3**). Obtained results (**Fig. S6**) suggest that variations in the concentration of NPs in the graphene hybrid do not significantly impact the adsorption of the tested drugs, indicating that the net surface area for drug adsorption of hybrids is comparable to that of unmodified graphene. Therefore, the minor variations in the adsorption observed values has been ascribed to differences in solubility, maybe due to the increased weight of NP-loaded graphene[57-58].

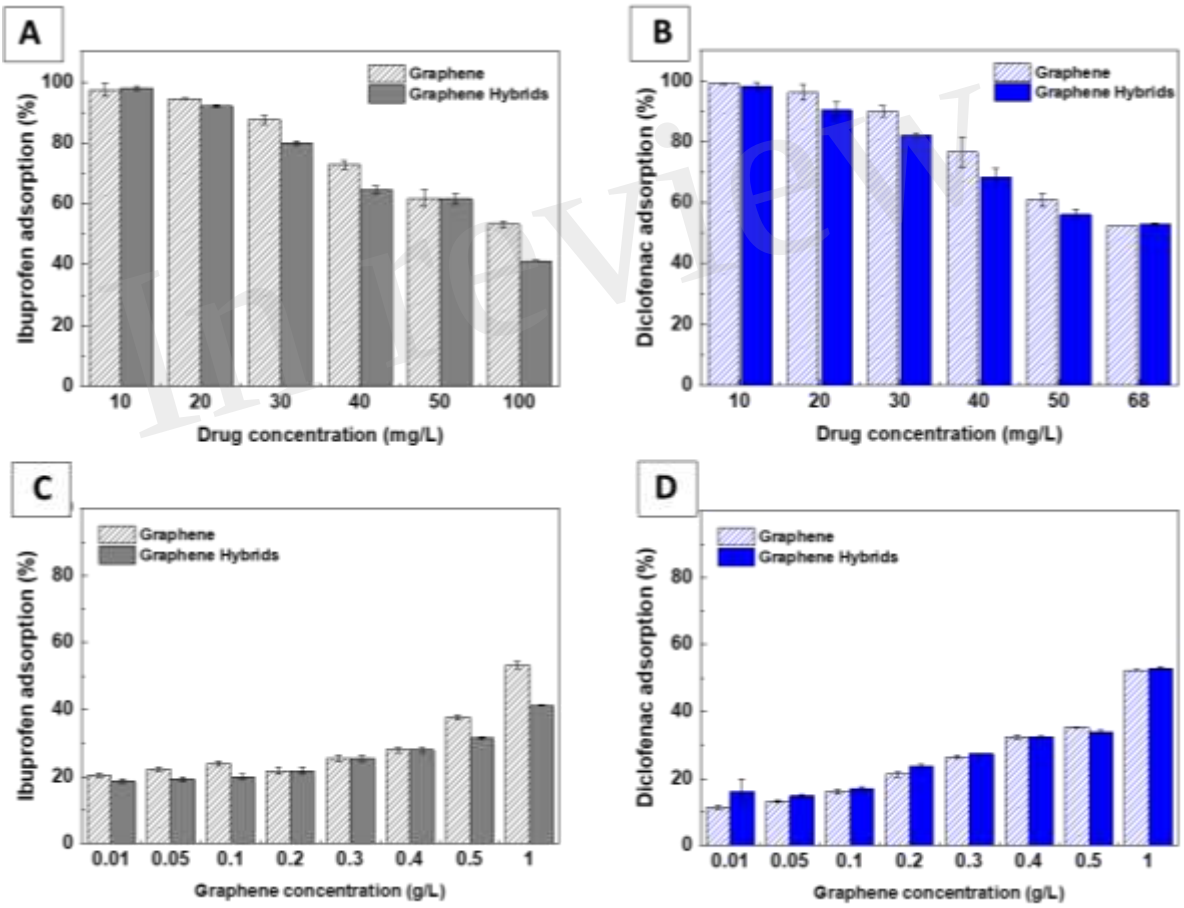

Figure 5. **Adsorption isotherms of Graphene and Graphene hybrids.** Adsorption of IBP (A) and DCF solutions (B) at different drug concentrations exposed to Graphene / Fe_3O_4 hybrids ($3.2 \cdot 10^{15}$ NPs/g graphene; 1 g/L graphene). Adsorption of IBP (C) and DCF (D) (EC_{50} concentrations) exposed to varying concentrations of Graphene / Fe_3O_4 hybrids ($3.2 \cdot 10^{15}$ NPs/g Graphene) and Graphene.

The absorption affinity onto graphene of organic molecules in water ultimately depends on charge distribution, hydrophobicity and hydrophilicity. Therefore, we tested if more hydrophilic graphene oxide (GO) would be more or less soluble and absorb more or less drug. The same experiments were performed with GO synthesized via a modified Hummer's method:[59] oxidation under acidic conditions at room temperature for 6 days. An aliquot was taken on the 3rd day of the experiment. Samples were thoroughly washed, concentrated at 1g/L were characterized by Electron Microscopy and FT-IR, to confirm the oxidation of graphene.

Fig. 6A-B shows a low magnification image of GO hybrid nanoestructures obtained after 3 days and 6 days. In both cases, the NPs can be resolved against the weak background of the GO sheet. Consistent with oxidation, FTIR spectrum of GO samples shows the characteristic vibration peaks allocated to O-H stretching, C=O stretching, and C-O stretching, which agrees well with commercial GO and previous works[60-61]. The broad peak at 3.434 cm^{-1} is assigned to OH groups and reveals the presence of hydroxy groups in GO. The band observed at 1.726 cm^{-1} is assigned to the carboxyl group, which would facilitate the attachment of NPs through electrostatic interaction[61]. The sharp peak found at 1.627 cm^{-1} corresponds to the stretching and bending vibration of OH groups of water molecules adsorbed on GO. The FT-IR spectrum of Fe_3O_4 and TiO_2 NPs shows the characteristic absorption bands around 3450 cm^{-1} assigned to stretching and 1630 cm^{-1} to bending vibration of O-H, representing the water as moisture. The intense peak around below 1000 cm^{-1} is assigned to the Fe-O and Ti-O stretching bands. Finally, a stable suspension of brown GO nanosheets was obtained, which presents a solid magnetic response to a permanent magnet (**Fig 6D, inset**).

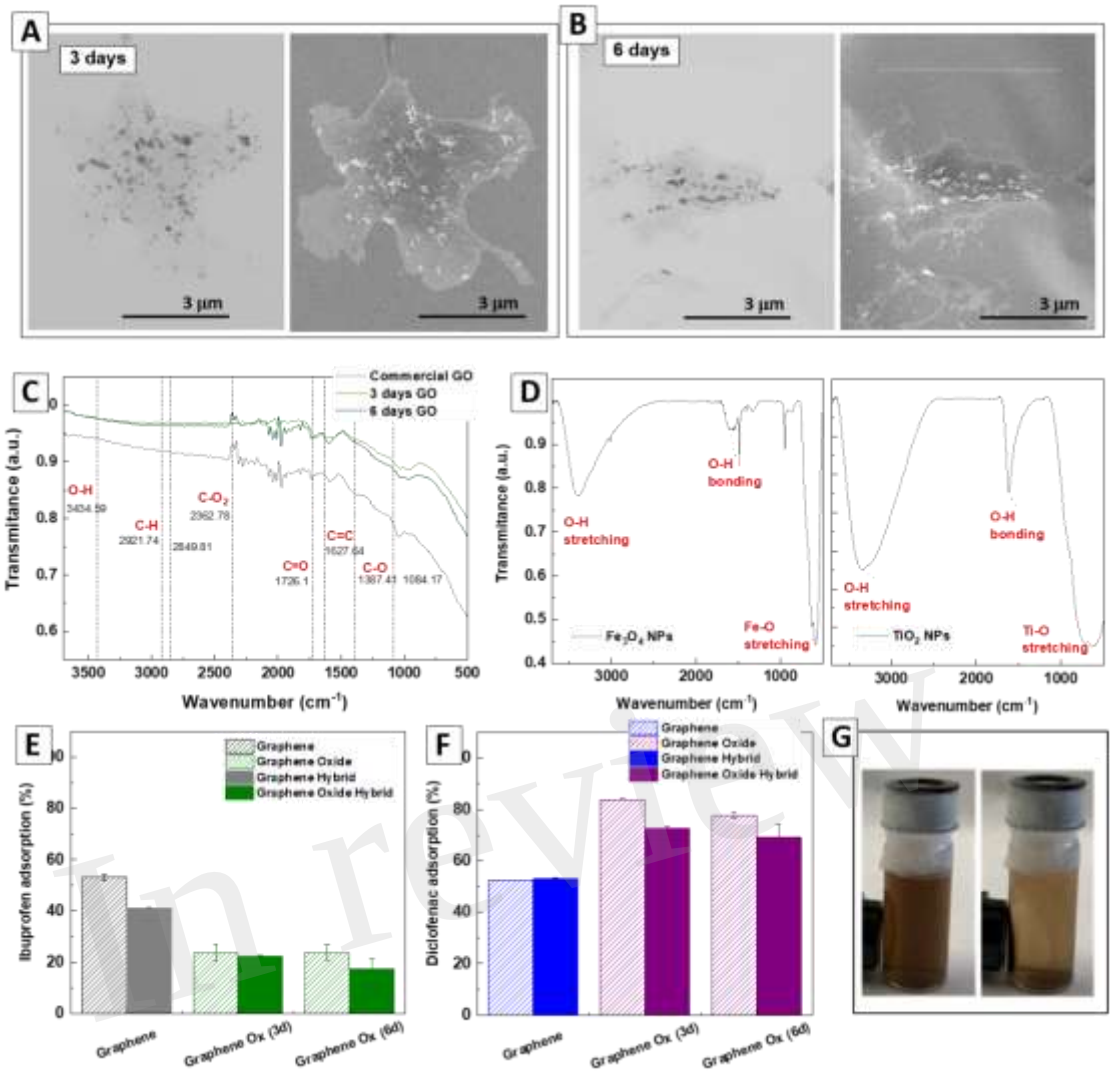

Figure 6. Transmission and Scanning Electron Microscopy of the Fe_3O_4/Graphene Oxide hybrid after 3 days (A) and 6 days (B) of oxidation under acidic conditions. FT-IR of the used graphene oxide (C) and the corresponding Fe_3O_4 and TiO_2 NPs. Adsorption of IBP (E) and DCF (F) in Graphene Oxide hybrids and controls. Image of a stable suspension of brown GO nanosheets, which presents a solid magnetic response to a permanent magnet (**G**).

Adsorption of IBP and DCF in GO hybrids and controls are shown in **Fig. 6D-E**. GO hybrid showed a notable decrease in adsorption when exposed to IBP and better results when exposed to DCF (**Fig. 6D-E**). This fact appears relatively independent of oxidation time, 3d o 6d. Graphene is reported to interact via π-π with the benzoic ring of both species while, in the case of GO, other intermolecular forces are introduced to the system, such as hydrogen bridges. These new interactions would explain the improvement of results in the case of DCF, which has free electrons in its structure (from the Cl- and the NH- groups), while results from IBP, with only a polar group, are worse.

The final performance of the hybrids was testing the photocatalytic degradation of adsorbed species. Photocatalysis is considered an effective system for destroying many organics by generating nonselective and highly oxidative oxygen species, reducing considerably the organic load of effluents,

using procedures with relatively low costs. Under UV light, highly photocatalytic TiO_2 NPs, with a bandgap of 3.2 eV, are activated, generating electron-hole pairs that then reduce oxygen or oxidize water to produce very reactive free radical species (such as HO• and O2•−) that are responsible for molecule degradation.[62-65] Remarkably, compared to pure TiO_2 NPs, the light absorbance of GM/Fe_3O_4/TiO_2 hybrid nanostructures is extended into the visible range, which is in faithful agreement with the colour of the samples (i.e., white for bare TiO_2 NPs and dark grey for composite hybrid material).

To test the effects of photocatalysis on the exposed samples, we first incubated them for 2 hours to the EC50 concentration of the studied drugs (100 mg/L and 68 mg/mL for the IBP and the DCF, respectively). Then, samples were purified magnetically and the supernatant was analyzed by UV-Vis spectroscopy (**Fig. 7, first exposition**) and Then, samples were purified, exposed to UV light for 2 hours, purified, and incubated again with drug solutions at the corresponding EC50 concentration. (**Fig. 7, second exposition**). The obtained results indicated that, compared to controls, the loading capacity of GM/Fe_3O_4/TiO_2 hybrid nanostructures increased after the samples' re-exposure, indicating the destruction of drugs. Evidence in the literature and ongoing investigations suggest that optimising regeneration conditions can increase the reusability of the structures[66-67].

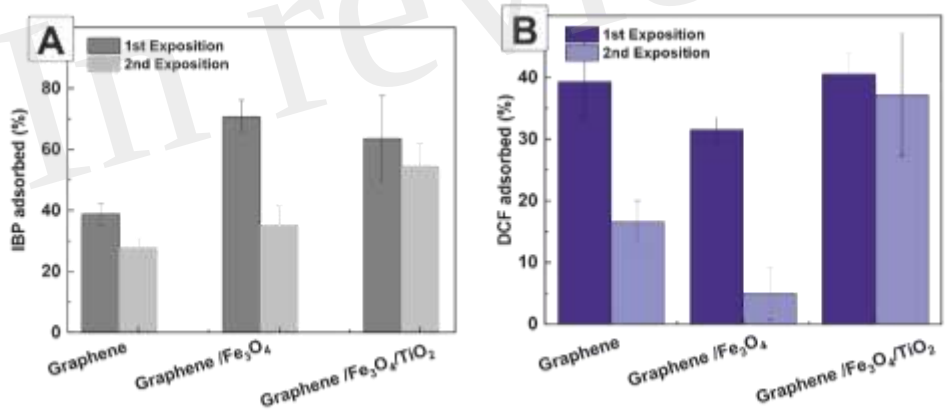

Figure 7. Photocatalytic degradation of adsorbed species by TiO_2 NPs Concentration of the studied drugs IBP (A) and DCF (B) after different hybrid configurations have been exposed to EC50 solutions. Significant error bars are the standard deviation of three completely independent samples (not replicates).

CONCLUSIONS

In this work, we have reported the simple and straight forward preparation of graphene-based magnetic and optically active hybrid materials by the adsorption of magnetite and titania nanoparticles. They are intended for their application in removing and degrading (seek and destroy) emerging persistent organic pollutants as anti-inflammatory drugs – such as IBP and DCF-. This materials are prepared by RT incubation of the NPs and the GM in surfactant depletion conditions. Modifications of the hybrid have been made, allowing us to understand i) the role of the functional groups at the surface and the polarity of the adsorbed species in the case of the Graphene Oxide and ii) the additive properties that can offer a multi-modal hybrid in the case of the hybrid nanostructures. The presence of magnetite allow for the efficient removal of the hybrid while the presence of photocatalytic titania allow to degrade the absorbed drugs opening the door for recycling of the hybrid.

EXPERIMENTALS

Materials.

Iron III Chloride ($FeCl_3$ anhydrous, powder, ≥99.99% trace metals basis), Iron(II) chloride tetrahydrate ($FeCl_2 \cdot 4H_2O$ puriss. p.a., ≥99.0% (RT)), stored in a glovebox under inert conditions, Diclofenac (DCF) and Tetramethylammonium hydroxide solution (TMAOH), Sodium Hydroxide (NaOH), Hydrochloric Acid (HCl) and Hydrogen Peroxide (30v/v) where purchased from Sigma-Aldrich and. Float-A-Lyzer devices of 0.5-1kDa were purchased from Spectrum Labs and used after activation with 10% Ethanol solution as described by the company. 4-Isobutyl-alpha-methylphenylacetic acid, 99% (Ibuprofen-IBP) was purchased from Alfa Aesar. Titanium Isopropoxide was purchased from Fluka. Graphene flakes were kindly donated by Arben Merkoçi group at ICN2. All chemicals were used as received without further purification. Distilled water passed through a Millipore system (ρ = 18.2 MΩ) was used in all experiments.

Synthesis of Fe_3O_4/graphene hybrids

Synthesis of Fe_3O_4 NPs: Synthesis of Fe_3O_4 magnetite NPs of ~7 nm has been performed following a previously reported method.[47,48] Briefly, in a 250mL round bottom flask, 1.824g of $FeCl_3$ anhydrous and 0.996g of $FeCl_2 \cdot 4H_2O$ are sequentially added to 50 mL of mQ water deoxygenated under N_2 bubbling for 30 minutes and stirred until complete dissolution. Afterwards, 50mL of 1M TMAOH previously deoxygenated under N_2 bubbling for 30 minutes is poured continuously onto the solution containing the Fe(II) and Fe(III) precursors stirred at 600rpm under Nitrogen atmosphere. The mixture is left stirring for 30min. Once the reaction is completed the sample is washed twice by magnetically aided sedimentation and finally resuspended in 10mM TMAOH. Sample is stored under nitrogen atmosphere to avoid its degradation.

Synthesis of TiO_2 NPs: Synthesis of TiO_2 anatase NPs of ~4 nm has been performed following a previously reported method.[49] Briefly, NaOH 3M and HCl 3M solutions were prepared. Afterwards, 2.07mL of Titanium Isopropoxide were added to the 10 mL of the acid solution. Once the solution was homogeneous, 30mL of mQ water and 5mL of the base solution were carefully added to the solution containing the Titanium precursor, pH was then adjusted to pH 5. The solution was left covered in an oven at 70ºC without stirring for 24h. The resulting nanoparticles were centrifuged twice, the first time at 500g and the second one at 1000g and resuspended in water. Afterwards, they were thoroughly sonicated in a sonics bath for several hours, centrifuged at 1000g and resuspended in 10mM TMAOH.

Post-synthesis procedure, preparation of the hybrid: For the attachment of NPs to the graphene structure a calculated amount of $2 \cdot 10^{12}$NPs (see S2 for calculations) were mixed with 625µL of 5mg/mL suspension of Graphene in H_2O ($3.2 \cdot 10^{12}$NPs/mg graphene) and dialyzed versus H_2O in 0.5-1kDa, 5mL dialysis bags for 3 days, constantly stirred and renewing the dialysis water twice per day. After the procedure was completed, the dialyzed samples were precipitated under 2000g centrifugation for 10

minutes and the supernatant containing non-attached crystals was removed and replaced with 5mL Milli-Q-Water, this process was performed twice. In the case of Fe_3O_4-TiO_2/Graphene hybrids, TiO_2 NPs were added to the dialysis bag after the afformentioned process was completed and decoration was accomplished by following the same steps. TiO_2 NPs were washed prior to dialysis via centrifugation and the pellet was re-suspended in water. Study of the deposition mechanism and the hybrid formation control was performed by synthesis of the hybrid at different and defined Graphene-to-Nanocrystal ratios. Concentrations of NPs were calculated by taking in account the size, composition and concentration of precursors in the original synthesis, as well as its yield. This process was easily scalable and for the following experiments, 3.75mL of Graphene suspension were used per each synthesis.

Synthesis of graphene oxide: Synthesis of graphene oxide was performed by adaptation of a simplified Hummer's method previously reported in the literature.[50] Briefly, 0.5g of graphene flakes were mixed with 66.5mL of H_2SO_4 in a 250mL cooled by an ice bath. Afterward, 3g of $KMnO_4$ were slowly added under vigorous stirring, at this point the solution was purplish green. Solution was left stirring for 3 and 6 days capped and it gradually turned to a deep green color. After this time had passed, the solution was poured in a 500mL flask containing 66.5mL of cold Mili-Q Water, this reaction was exothermic and effervescent and the solution turned to a reddish brown color. Finally, 4.5mL of H_2O_2 were added and the solution was left stirring for 10 minutes, turning to a light yellow color. The final graphene oxide solution was washed 3 times centrifuging at 10000g for 15 minutes and replacing the supernatant with 3M HCl in order to remove the metal impurities that may had remained, finally the centrifugation process was repeated, replacing the supernatant with Mili-Q Water until the pH of the solution was 4-5.

Techniques

UV–Vis Spectroscopy: UV–visible spectra were acquired with a Cary 60 spectrophotometer. Measurements were performed using a quartz cuvette with a 10 mm light pathway in the 200–800 nm range at room temperature.

Transmission Electron Microscopy: The morphology of the Fe_3O_4/Graphene hybrids were visualized using FEI Magellan 400L XHR SEM, in transmission mode operated at 20 kV. Morphology of Fe_3O_4NPs was observed using a FEI Tecnai G2 F20 HR(S)TEM operated at 200kV in Bright Field mode. A droplet (10µL) of the sample after 5 minute ultrasonication of a 1:5 dilution of the samples was drop cast onto a piece of ultrathin carbon-coated 200-mesh copper grid (Ted-pella, Inc.) and left to dry in air.

SQUID measurements: The magnetic behaviour of the hybrid was evaluated via SQUID magnetometry and hysteresis loops observed at 10K and 300K.

Termogravimetric analysis (TGA): For termogravimetric analysis was heated from 25ºC to a final temperature of 900ºC at a 10ºC/min rate under an air flow of 24mL/min.

Acknowledgements

We acknowledge financial support from the Spanish Ministerio de Ciencia, Innovación y Universidades (MCIU) (RTI2018-099965-B-I00, AEI/FEDER,UE) proyectos de I+D+i de programación conjunta internacional MCIN/AEI (CONCORD, PCI2019-103436) cofunded by the European Union and Generalitat de Catalunya (2017-SGR-1431). ICN2 is supported by the Severo Ochoa program from Spanish MINECO (SEV-2017-0706) and is funded by the CERCA Programme/Generalitat de Catalunya.

REFRENCES

1. Karn, B.; Kuiken, T.; Otto, M., Nanotechnology and in situ remediation: a review of the benefits and potential risks. *Environ Health Perspect* **2009,** *117* (12), 1813-31.

2. Shannon, M. A.; Bohn, P. W.; Elimelech, M.; Georgiadis, J. G.; Mariñas, B. J.; Mayes, A. M., Science and technology for water purification in the coming decades. *Nature* **2008,** *452* (7185), 301-310.

3. Stackelberg, P. E.; Furlong, E. T.; Meyer, M. T.; Zaugg, S. D.; Henderson, A. K.; Reissman, D. B., Persistence of pharmaceutical compounds and other organic wastewater contaminants in a conventional drinking-water-treatment plant. *Sci Total Environ* **2004,** *329* (1-3), 99-113.

4. Daughton, C. G.; Ternes, T. A., Pharmaceuticals and personal care products in the environment: agents of subtle change? *Environ Health Perspect* **1999,** *107 Suppl 6* (Suppl 6), 907-38.

5. Taheran, M.; Naghdi, M.; Brar, S. K.; Verma, M.; Surampalli, R. Y., Emerging contaminants: Here today, there tomorrow! *Environmental Nanotechnology, Monitoring & Management* **2018,** *10*, 122-126.

6. Kümmerer, K., Drugs in the environment: emission of drugs, diagnostic aids and disinfectants into wastewater by hospitals in relation to other sources--a review. *Chemosphere* **2001,** *45* (6-7), 957-69.

7. Kümmerer, K., Pharmaceuticals in the Environment – A Brief Summary. In *Pharmaceuticals in the Environment: Sources, Fate, Effects and Risks*, Kümmerer, K., Ed. Springer Berlin Heidelberg: Berlin, Heidelberg, 2008; pp 3-21.

8. Patel, M.; Kumar, R.; Kishor, K.; Mlsna, T.; Pittman, C. U.; Mohan, D., Pharmaceuticals of Emerging Concern in Aquatic Systems: Chemistry, Occurrence, Effects, and Removal Methods. *Chemical Reviews* **2019,** *119* (6), 3510-3673.

9. Wilkinson, J. L.; Boxall, A. B. A.; Kolpin, D. W.; Leung, K. M. Y.; Lai, R. W. S.; Galbán-Malagón, C.; Adell, A. D.; Mondon, J.; Metian, M.; Marchant, R. A.; Bouzas-Monroy, A.; Cuni-Sanchez, A.; Coors, A.; Carriquiriborde, P.; Rojo, M.; Gordon, C.; Cara, M.; Moermond, M.; Luarte, T.; Petrosyan, V.; Perikhanyan, Y.; Mahon, C. S.; McGurk, C. J.; Hofmann, T.; Kormoker, T.; Iniguez, V.; Guzman-Otazo, J.; Tavares, J. L.; Figueiredo, F. G. D.; Razzolini, M. T. P.; Dougnon, V.; Gbaguidi, G.; Traoré, O.; Blais, J. M.; Kimpe, L. E.; Wong, M.; Wong, D.; Ntchantcho, R.; Pizarro, J.; Ying, G.-G.; Chen, C.-E.; Páez, M.; Martínez-Lara, J.; Otamonga, J.-P.; Poté, J.; Ifo, S. A.; Wilson, P.; Echeverría-Sáenz, S.; Udikovic-Kolic, N.; Milakovic, M.; Fatta-Kassinos, D.; Ioannou-Ttofa, L.; Belušová, V.; Vymazal, J.; Cárdenas-Bustamante, M.; Kassa, B. A.; Garric, J.; Chaumot, A.; Gibba, P.; Kunchulia, I.; Seidensticker, S.; Lyberatos, G.; Halldórsson, H. P.; Melling, M.; Shashidhar, T.; Lamba, M.; Nastiti, A.; Supriatin, A.; Pourang, N.; Abedini, A.; Abdullah, O.; Gharbia, S. S.; Pilla, F.; Chefetz, B.; Topaz, T.; Yao, K. M.; Aubakirova, B.; Beisenova, R.; Olaka, L.; Mulu, J. K.; Chatanga, P.; Ntuli, V.; Blama, N. T.; Sherif, S.; Aris, A. Z.; Looi, L. J.; Niang, M.; Traore, S. T.; Oldenkamp, R.; Ogunbanwo, O.; Ashfaq, M.; Iqbal, M.; Abdeen, Z.; O'Dea, A.; Morales-Saldaña, J. M.; Custodio, M.; Cruz, H. d. l.; Navarrete, I.; Carvalho, F.; Gogra, A. B.; Koroma, B. M.; Cerkvenik-Flajs, V.; Gombač, M.; Thwala, M.; Choi, K.; Kang, H.; Ladu, J. L. C.; Rico, A.; Amerasinghe, P.; Sobek, A.; Horlitz, G.; Zenker, A. K.; King, A. C.; Jiang, J.-J.; Kariuki, R.; Tumbo, M.; Tezel, U.; Onay, T. T.; Lejju, J. B.; Vystavna, Y.; Vergeles, Y.; Heinzen, H.; Pérez-Parada, A.; Sims, D. B.; Figy, M.; Good, D.; Teta, C., Pharmaceutical pollution of the world’s rivers. *Proceedings of the National Academy of Sciences* **2022,** *119* (8), e2113947119.

10. de Voogt, P.; Janex-Habibi, M.-L.; Sacher, F.; Puijker, L.; Mons, M., Development of a common priority list of pharmaceuticals relevant for the water cycle. *Water Science and Technology* **2009,** *59* (1), 39-46.

11. Zhou, J. L.; Zhang, Z. L.; Banks, E.; Grover, D.; Jiang, J. Q., Pharmaceutical residues in wastewater treatment works effluents and their impact on receiving river water. *J Hazard Mater* **2009,** *166* (2-3), 655-61.

12. Ginebreda, A.; Muñoz, I.; de Alda, M. L.; Brix, R.; López-Doval, J.; Barceló, D., Environmental risk assessment of pharmaceuticals in rivers: Relationships between hazard indexes and aquatic macroinvertebrate diversity indexes in the Llobregat River (NE Spain). *Environment International* **2010,** *36* (2), 153-162.

13. Godfrey, E.; Woessner, W. W.; Benotti, M. J., Pharmaceuticals in on-site sewage effluent and ground water, Western Montana. *Ground Water* **2007,** *45* (3), 263-71.

14. Heckmann, L. H.; Callaghan, A.; Hooper, H. L.; Connon, R.; Hutchinson, T. H.; Maund, S. J.; Sibly, R. M., Chronic toxicity of ibuprofen to Daphnia magna: Effects on life history traits and population dynamics. *Toxicol Lett* **2007,** *172* (3), 137-45.

15. Du, J.; Mei, C. F.; Ying, G. G.; Xu, M. Y., Toxicity Thresholds for Diclofenac, Acetaminophen and Ibuprofen in the Water Flea Daphnia magna. *Bull Environ Contam Toxicol* **2016,** *97* (1), 84-90.

16. Parolini, M.; Binelli, A., Sub-lethal effects induced by a mixture of three non-steroidal anti-inflammatory drugs (NSAIDs) on the freshwater bivalve Dreissena polymorpha. *Ecotoxicology* **2012,** *21* (2), 379-92.

17. Kaur, A.; Umar, A.; Kansal, S. K., Heterogeneous photocatalytic studies of analgesic and non-steroidal anti-inflammatory drugs. *Applied Catalysis A: General* **2016,** *510*, 134-155.

18. Khan, S. J.; Wintgens, T.; Sherman, P.; Zaricky, J.; Schäfer, A. I., Removal of hormones and pharmaceuticals in the Advanced Water Recycling Demonstration Plant in Queensland, Australia. *Water Sci Technol* **2004,** *50* (5), 15-22.

19. Suarez, S.; Lema, J. M.; Omil, F., Pre-treatment of hospital wastewater by coagulation-flocculation and flotation. *Bioresource Technology* **2009,** *100* (7), 2138-46.

20. Langenhoff, A.; Inderfurth, N.; Veuskens, T.; Schraa, G.; Blokland, M.; Kujawa-Roeleveld, K.; Rijnaarts, H., Microbial Removal of the Pharmaceutical Compounds Ibuprofen and Diclofenac from Wastewater. *BioMed Research International* **2013,** *2013*, 325806.

21. Ahmed, M. J., Adsorption of non-steroidal anti-inflammatory drugs from aqueous solution using activated carbons: Review. *Journal of Environment Management* **2017,** *190*, 274-282.

22. Mlunguza, N. Y.; Ncube, S.; Nokwethemba Mahlambi, P.; Chimuka, L.; Madikizela, L. M., Adsorbents and removal strategies of non-steroidal anti-inflammatory drugs from contaminated water bodies. *Journal of Environmental Chemical Engineering* **2019,** *7* (3), 103142.

23. Kanakaraju, D.; Glass, B. D.; Oelgemöller, M., Advanced oxidation process-mediated removal of pharmaceuticals from water: A review. *Journal of Environmental Management* **2018,** *219*, 189-207.

24. Feng, L.; van Hullebusch, E. D.; Rodrigo, M. A.; Esposito, G.; Oturan, M. A., Removal of residual anti-inflammatory and analgesic pharmaceuticals from aqueous systems by electrochemical advanced oxidation processes. A review. *Chemical Engineering Journal* **2013,** *228*, 944-964.

25. Villanueva-Rodríguez, M.; Bello-Mendoza, R.; Hernández-Ramírez, A.; Ruiz-Ruiz, E. J., Degradation of anti-inflammatory drugs in municipal wastewater by heterogeneous photocatalysis and electro-Fenton process. *Environmental Technology* **2019,** *40* (18), 2436-2445.

26. Ternes, T. A.; Stuber, J.; Herrmann, N.; McDowell, D.; Ried, A.; Kampmann, M.; Teiser, B., Ozonation: a tool for removal of pharmaceuticals, contrast media and musk fragrances from wastewater? *Water Res* **2003,** *37* (8), 1976-82.

27. Zhu, Y.; Murali, S.; Cai, W.; Li, X.; Suk, J. W.; Potts, J. R.; Ruoff, R. S., Graphene and graphene oxide: synthesis, properties, and applications. *Adv Mater* **2010,** *22* (35), 3906-24.

28. Chandra, V.; Park, J.; Chun, Y.; Lee, J. W.; Hwang, I. C.; Kim, K. S., Water-dispersible magnetite-reduced graphene oxide composites for arsenic removal. *ACS Nano* **2010,** *4* (7), 3979-86.

29. Maliyekkal, S. M.; Sreeprasad, T. S.; Krishnan, D.; Kouser, S.; Mishra, A. K.; Waghmare, U. V.; Pradeep, T., Graphene: a reusable substrate for unprecedented adsorption of pesticides. *Small* **2013,** *9* (2), 273-83.

30. Al-Khateeb, L. A.; Almotiry, S.; Salam, M. A., Adsorption of pharmaceutical pollutants onto graphene nanoplatelets. *Chemical Engineering Journal* **2014,** *248*, 191-199.

31. Chen, L.; Li, Y.; Hu, S.; Sun, J.; Du, Q.; Yang, X.; Ji, Q.; Wang, Z.; Wang, D.; Xia, Y., Removal of methylene blue from water by cellulose/graphene oxide fibres. *Journal of experimental Nanoscience* **2016,** *11* (14), 1156-1170.

32. Gul, A.; Khaligh, N. G.; Julkapli, N. M., Surface modification of carbon-based nanoadsorbents for the advanced wastewater treatment. *Journal of Molecular Structure* **2021,** *1235*, 130148.

33. Guerra, F. D.; Attia, M. F.; Whitehead, D. C.; Alexis, F., Nanotechnology for Environmental Remediation: Materials and Applications. *Molecules* **2018,** *23* (7), 1760.

34. Sun, H.; Cao, L.; Lu, L., Magnetite/reduced graphene oxide nanocomposites: One step solvothermal synthesis and use as a novel platform for removal of dye pollutants. *Nano Research* **2011,** *4* (6), 550-562.

35. Shan, D.; Deng, S.; Jiang, C.; Chen, Y.; Wang, B.; Wang, Y.; Huang, J.; Yu, G.; Wiesner, M. R., Hydrophilic and strengthened 3D reduced graphene oxide/nano-Fe3O4 hybrid hydrogel for enhanced adsorption and catalytic oxidation of typical pharmaceuticals. *Environmental Science: Nano* **2018,** *5* (7), 1650-1660.

36. Mendez-Arriaga, F.; Esplugas, S.; Gimenez, J., Photocatalytic degradation of non-steroidal anti-inflammatory drugs with TiO2 and simulated solar irradiation. *Water Res* **2008,** *42* (3), 585-94.

37. Romeiro, A.; Azenha, M. E.; Canle, M.; Rodrigues, V. H. N.; Da Silva, J. P.; Burrows, H. D., Titanium Dioxide Nanoparticle Photocatalysed Degradation of Ibuprofen and Naproxen in Water: Competing Hydroxyl Radical Attack and Oxidative Decarboxylation by Semiconductor Holes. *Chemistryselect* **2018,** *3* (39), 10915-10924.

38. Nam, S. W.; Jung, C.; Li, H.; Yu, M.; Flora, J. R.; Boateng, L. K.; Her, N.; Zoh, K. D.; Yoon, Y., Adsorption characteristics of diclofenac and sulfamethoxazole to graphene oxide in aqueous solution. *Chemosphere* **2015,** *136*, 20-6.

39. Khalil, A. M. E.; Memon, F. A.; Tabish, T. A.; Salmon, D.; Zhang, S.; Butler, D., Nanostructured porous graphene for efficient removal of emerging contaminants (pharmaceuticals) from water. *Chemical Engineering Journal* **2020,** *398*, 125440.

40. Hiew, B. Y. Z.; Lee, L. Y.; Lee, X. J.; Gan, S.; Thangalazhy-Gopakumar, S.; Lim, S. S.; Pan, G.-T.; Yang, T. C.-K., Adsorptive removal of diclofenac by graphene oxide: Optimization, equilibrium, kinetic and thermodynamic studies. *Journal of the Taiwan Institute of Chemical Engineers* **2019,** *98*, 150-162.

41. Shan, D.; Deng, S.; Li, J.; Wang, H.; He, C.; Cagnetta, G.; Wang, B.; Wang, Y.; Huang, J.; Yu, G., Preparation of porous graphene oxide by chemically intercalating a rigid molecule for enhanced removal of typical pharmaceuticals. *Carbon* **2017,** *119*, 101-109.

42. Shen, J.; Hu, Y.; Shi, M.; Li, N.; Ma, H.; Ye, M., One Step Synthesis of Graphene Oxide−Magnetic Nanoparticle Composite. *The Journal of Physical Chemistry C* **2010,** *114* (3), 1498-1503.

43. Yang, X.; Zhang, X.; Ma, Y.; Huang, Y.; Wang, Y.; Chen, Y., Superparamagnetic graphene oxide–Fe3O4 nanoparticles hybrid for controlled targeted drug carriers. *Journal of Materials Chemistry* **2009,** *19* (18), 2710.

44. Cong, H. P.; He, J. J.; Lu, Y.; Yu, S. H., Water-soluble magnetic-functionalized reduced graphene oxide sheets: in situ synthesis and magnetic resonance imaging applications. *Small* **2010,** *6* (2), 169-73.

45. Su, J.; Cao, M.; Ren, L.; Hu, C., Fe3O4–Graphene Nanocomposites with Improved Lithium Storage and Magnetism Properties. *The Journal of Physical Chemistry C* **2011,** *115* (30), 14469-14477.

46. He, F.; Fan, J.; Ma, D.; Zhang, L.; Leung, C.; Chan, H. L., The attachment of Fe3O4 nanoparticles to graphene oxide by covalent bonding. *Carbon* **2010,** *48* (11), 3139-3144.

47. Li, Y.; Chu, J.; Qi, J.; Li, X., An easy and novel approach for the decoration of graphene oxide by Fe3O4 nanoparticles. *Applied Surface Science* **2011,** *257* (14), 6059-6062.

48. He, H.; Gao, C., Supraparamagnetic, conductive, and processable multifunctional graphene nanosheets coated with high-density Fe3O4 nanoparticles. *ACS Appl Mater Interfaces* **2010,** *2* (11), 3201-10.

49. Tran, B. T.; Tran, T. N.; Tran, A. M. T.; Nguyen, G. C. D.; Nguyen, Q. T. T., Simultaneous Determination of Paracetamol, Ibuprofen, and Caffeine in Tablets by Molecular Absorption Spectroscopy Combined with Classical Least Square Method. *Molecules* **2022,** *27* (9), 2657.

50. Marcon, L.; Oliveras, J.; Puntes, V. F., In situ nanoremediation of soils and groundwaters from the nanoparticle's standpoint: A review. *Sci Total Environ* **2021,** *791*, 148324.

51. Ventosa, M.; Oliveras, J.; Bastús, N. G.; Gimbert-Suriñach, C.; Puntes, V.; Llobet, A., Nanocrystal–Molecular Hybrids for the Photocatalytic Oxidation of Water. *ACS Applied Energy Materials* **2020,** *3* (10), 10008-10014.

52. Casals, E.; Barrena, R.; Garcia, A.; Gonzalez, E.; Delgado, L.; Busquets-Fite, M.; Font, X.; Arbiol, J.; Glatzel, P.; Kvashnina, K.; Sanchez, A.; Puntes, V., Programmed iron oxide nanoparticles disintegration in anaerobic digesters boosts biogas production. *Small* **2014,** *10* (14), 2801-8, 2741.

53. Recillas, S.; Garcia, A.; Gonzalez, E.; Casals, E.; Puntes, V.; Sanchez, A.; Font, X., Use of CeO2, TiO2 and Fe3O4 nanoparticles for the removal of lead from water: Toxicity of nanoparticles and derived compounds. *Desalination* **2010,** *277* (1-3), 213-220.

54. Dar, M. I.; Shivashankar, S. A., Single crystalline magnetite, maghemite, and hematite nanoparticles with rich coercivity. *RSC Adv.* **2014,** *4* (8), 4105-4113.

55. Jauris, I. M.; Matos, C. F.; Saucier, C.; Lima, E. C.; Zarbin, A. J.; Fagan, S. B.; Machado, F. M.; Zanella, I., Adsorption of sodium diclofenac on graphene: a combined experimental and theoretical study. *Phys Chem Chem Phys* **2016,** *18* (3), 1526-36.

56. Cleuvers, M., Mixture toxicity of the anti-inflammatory drugs diclofenac, ibuprofen, naproxen, and acetylsalicylic acid. *Ecotoxicology and Environment Safety* **2004,** *59* (3), 309-15.

57. Talbot, D.; Queiros Campos, J.; Checa-Fernandez, B. L.; Marins, J. A.; Lomenech, C.; Hurel, C.; Godeau, G. D.; Raboisson-Michel, M.; Verger-Dubois, G.; Obeid, L.; Kuzhir, P.; Bee, A., Adsorption of Organic Dyes on Magnetic Iron Oxide Nanoparticles. Part I: Mechanisms and Adsorption-Induced Nanoparticle Agglomeration. *ACS Omega* **2021,** *6* (29), 19086-19098.

58. Gutierrez, A. M.; Dziubla, T. D.; Hilt, J. Z., Recent advances on iron oxide magnetic nanoparticles as sorbents of organic pollutants in water and wastewater treatment. *Rev Environ Health* **2017,** *32* (1-2), 111-117.

59. Olumurewa, K. O.; Olofinjana, B.; Fasakin, O.; Eleruja, M. A.; Ajayi, E. O. B., Characterization of high yield graphene oxide synthesized by simplified hummers method. *Graphene* **2017,** *6* (4), 85-98.

60. Hayyan, M.; Abo-Hamad, A.; AlSaadi, M. A.; Hashim, M. A., Functionalization of graphene using deep eutectic solvents. *Nanoscale Res Lett* **2015,** *10* (1), 1004.

61. Rattana; Chaiyakun, S.; Witit-anun, N.; Nuntawong, N.; Chindaudom, P.; Oaew, S.; Kedkeaw, C.; Limsuwan, P., Preparation and characterization of graphene oxide nanosheets. *Procedia Engineering* **2012,** *32*, 759-764.

62. Guo, J.; Yuan, S.; Jiang, W.; Yue, H.; Cui, Z.; Liang, B., Adsorption and photocatalytic degradation behaviors of rhodamine dyes on surface-fluorinated TiO2 under visible irradiation. *RSC Advances* **2016,** *6* (5), 4090-4100.

63. Sousa, M. A.; Gonçalves, C.; Vilar, V. J. P.; Boaventura, R. A. R.; Alpendurada, M. F., Suspended TiO2-assisted photocatalytic degradation of emerging contaminants in a municipal WWTP effluent using a solar pilot plant with CPCs. *Chemical Engineering Journal* **2012,** *198-199*, 301-309.

64. Radjenović, J.; Sirtori, C.; Petrović, M.; Barceló, D.; Malato, S., Solar photocatalytic degradation of persistent pharmaceuticals at pilot-scale: Kinetics and characterization of major intermediate products. *Applied Catalysis B: Environmental* **2009,** *89* (1), 255-264.

65. Sheng, H.; Li, Q.; Ma, W.; Ji, H.; Chen, C.; Zhao, J., Photocatalytic degradation of organic pollutants on surface anionized TiO2: Common effect of anions for high hole-availability by water. *Applied Catalysis B: Environmental* **2013,** *138-139*, 212-218.

66. Li, C.; Xu, Q.; Xu, S.; Zhang, X.; Hou, X.; Wu, P., Synergy of adsorption and photosensitization of graphene oxide for improved removal of organic pollutants. *RSC Advances* **2017,** *7* (26), 16204-16209.

67. Gu, Y.; Yperman, J.; Carleer, R.; D'Haen, J.; Maggen, J.; Vanderheyden, S.; Vanreppelen, K.; Garcia, R. M., Adsorption and photocatalytic removal of Ibuprofen by activated carbon impregnated with TiO2 by UV–Vis monitoring. *Chemosphere* **2019,** *217*, 724-731.

Supplementary Information

Functionalization of Graphene Nanostructures with Inorganic Nanoparticles and Their Use for the Removal of Pharmaceutical Pollutants in Water

Jana Oliveras, Neus G. Bastús and Victor Puntes*

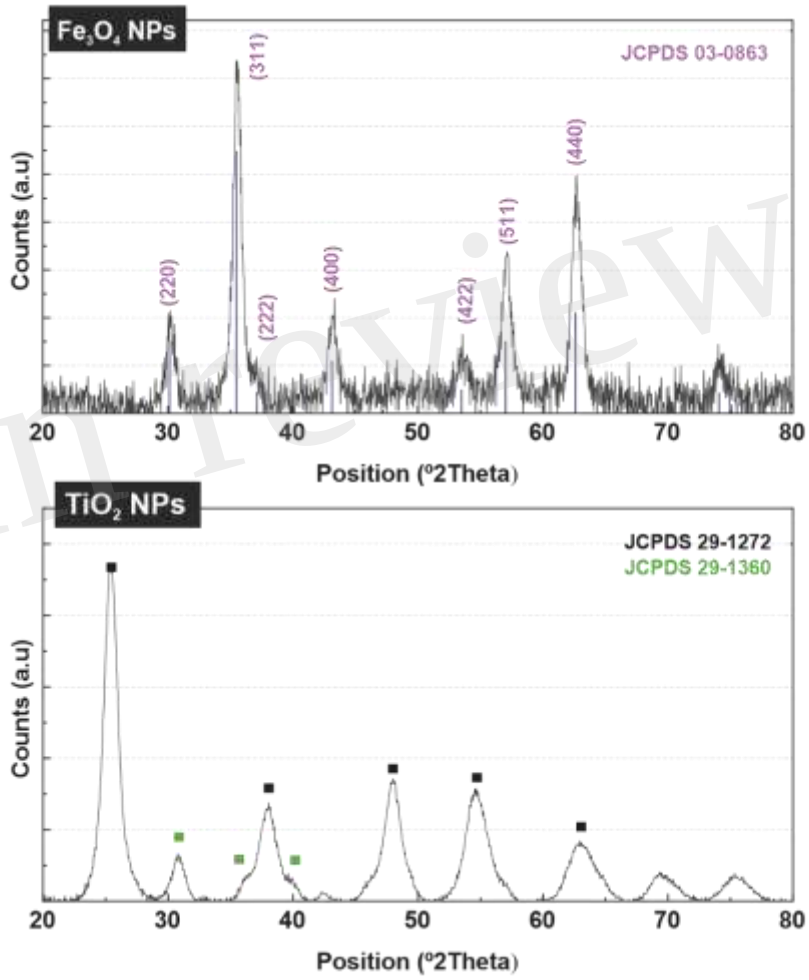

Figure S1. XRD patterns of the Fe_3O_4 and TiO_2 NPs and corresponding standard diffraction peaks of Fe_3O_4 (JCPDS card No. 03-0863) and TiO_2 (No. 29-1272 -anatase- and No. 29-1360 -brookite).

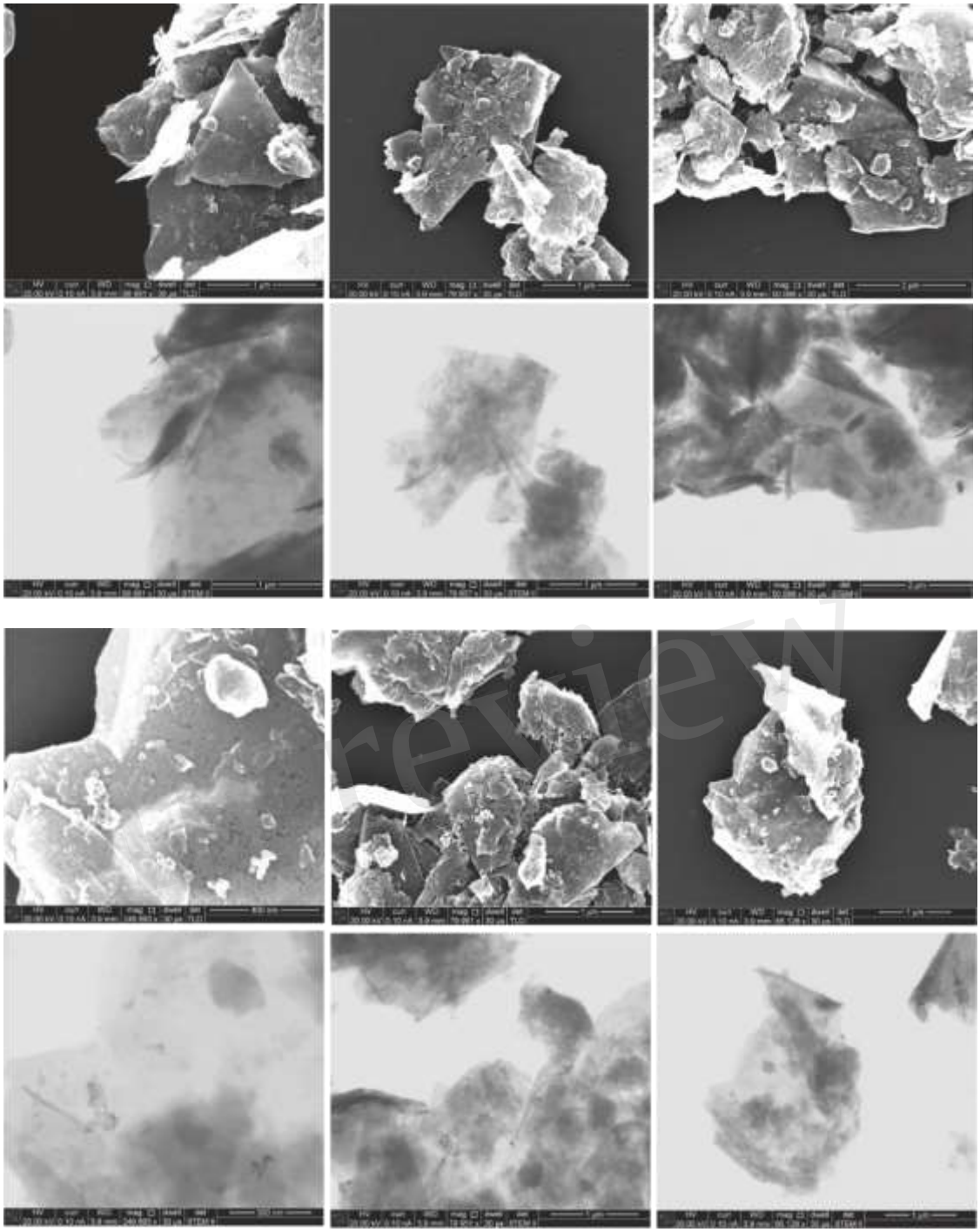

Figure S2. Scanning Electron Microscopy (SEM) and Scanning Transmission Electron Microscopy (STEM) of (TOP) Graphene/Fe_3O_4 hybrid nanostructures and (BOTTOM) of Graphene/Fe_3O_4/ TiO_2 hybrid nanostructures.

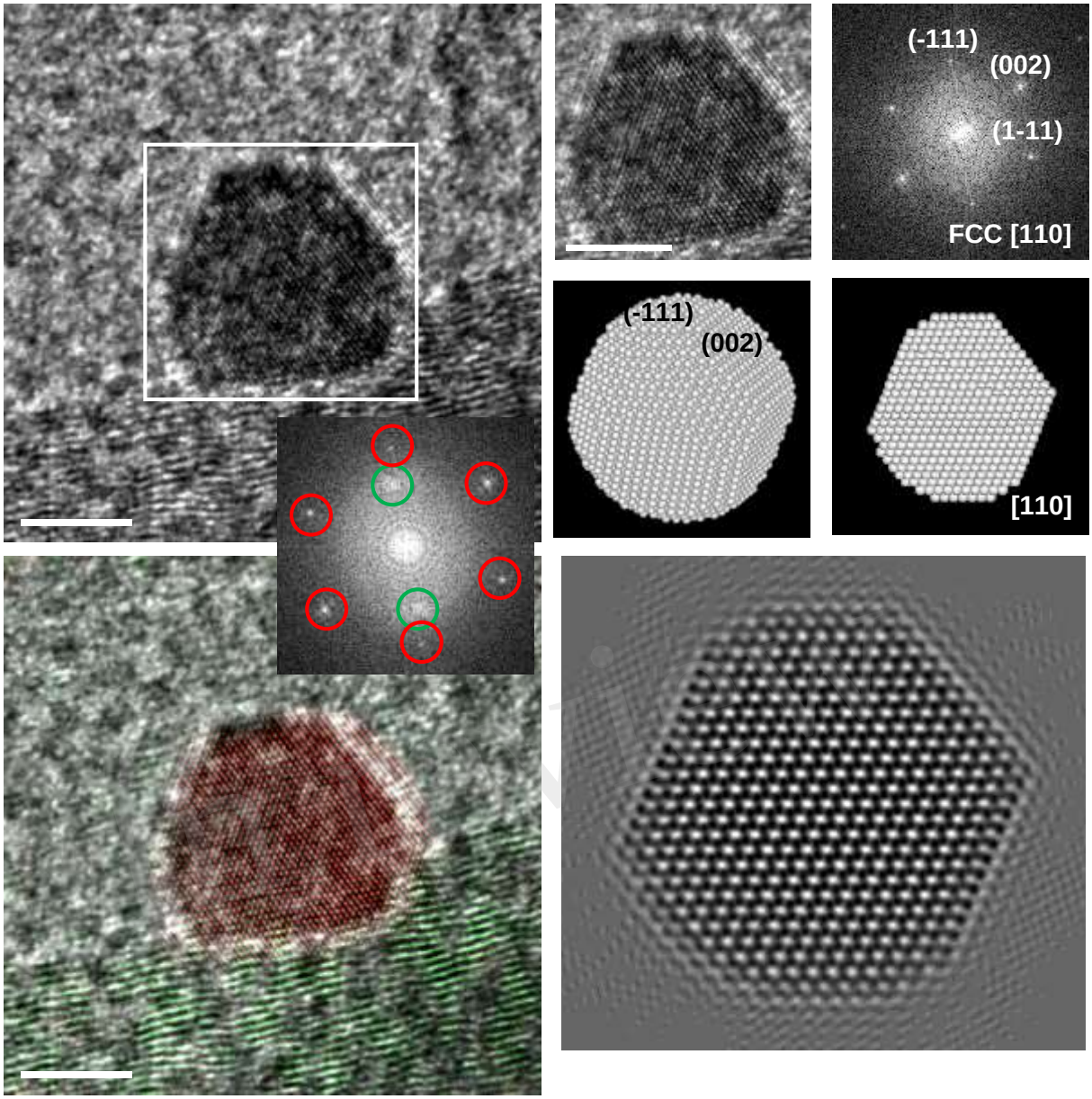

Figure S3. HRTEM image of the sample. On the top right, the coloured frequency filtered structural map where the different marked orientations are reported in different. On the bottom left: blow-up of the crystals in the white box and the corresponding indexed power spectrum. On the bottom right: a 3D atomic model reconstruction of the particle together with the TEM image simulation are reported.

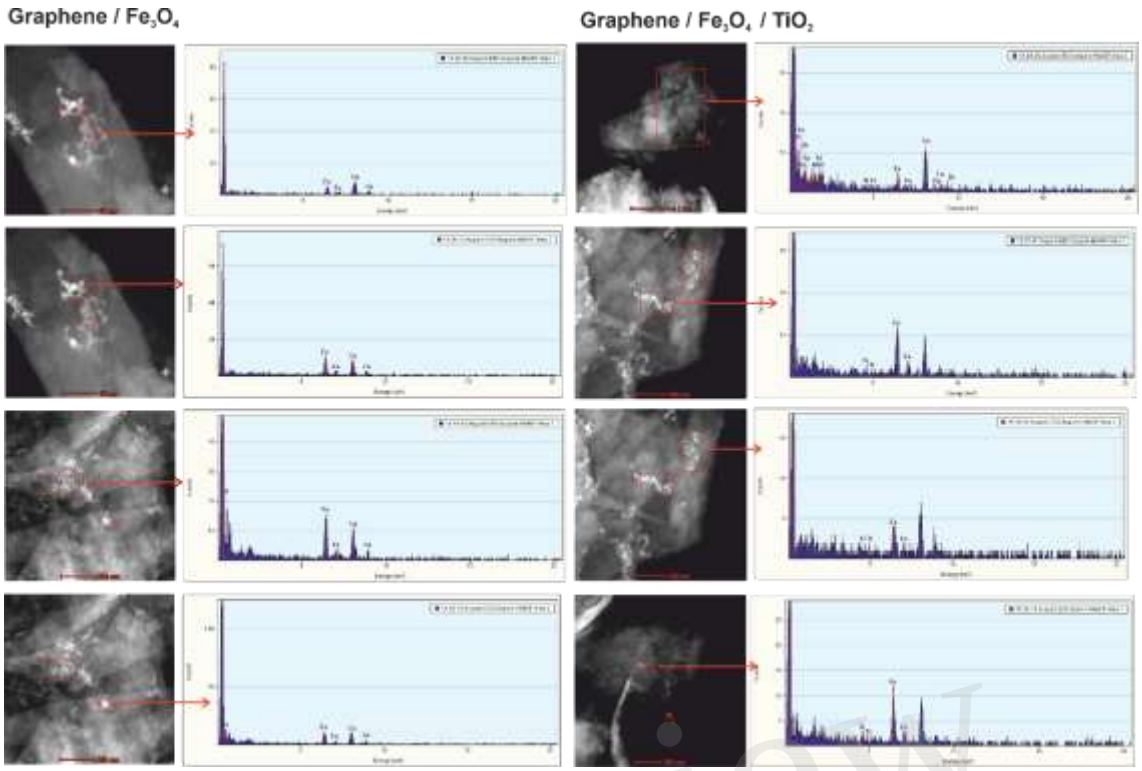

Figure S4. EDS analysis of the Graphene/Fe_3O_4 and Graphene/Fe_3O_4/ TiO_2 hybrid nanostructures. Scan profiles extracted from the representative sections of the HAADF-STEM images (as labelled) confirmed the presence of both types of NPs at the surface of the graphene sheet. The Cu peaks are the signal detected from the TEM grid.

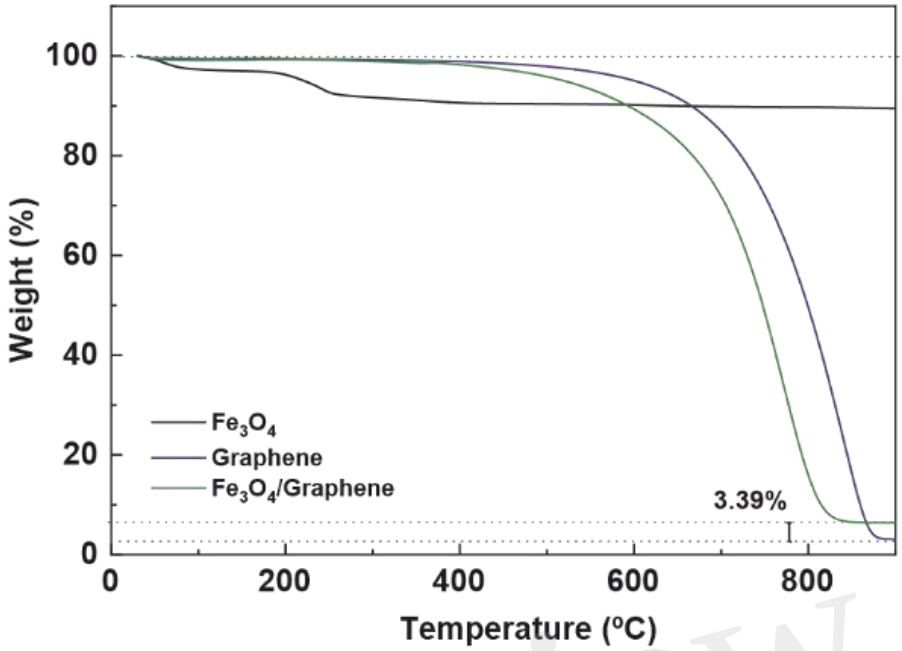

Figure S5. Termogravimetric curves of the Graphene-Fe_3O_4 samples.

Table S1. The concentration of pharmaceutical compounds was kept constant while that of graphene systematically varied.

Graphene] g/L	[IBP] mg/L	Fe_3O_4 NPs/g Graphene	Figure
0.01	100	$3.2 \cdot 10^{15}$	2-B1
0.05	100	$3.2 \cdot 10^{15}$	2-B1
0.1	100	$3.2 \cdot 10^{15}$	2-B1
0.2	100	$3.2 \cdot 10^{15}$	2-B1
0.3	100	$3.2 \cdot 10^{15}$	2-B1
0.4	100	$3.2 \cdot 10^{15}$	2-B1
0.5	100	$3.2 \cdot 10^{15}$	2-B1
1	100	$3.2 \cdot 10^{15}$	2-B1

EC50=100mg/L

Graphene] g/L	[IDCF] mg/L	Fe3O4 NPs/g Graphene	Figure
0.01	68	$3.2 \cdot 10^{15}$	2-B2
0.05	68	$3.2 \cdot 10^{15}$	2-B2
0.1	68	$3.2 \cdot 10^{15}$	2-B2
0.2	68	$3.2 \cdot 10^{15}$	2-B2
0.3	68	$3.2 \cdot 10^{15}$	2-B2
0.4	68	$3.2 \cdot 10^{15}$	2-B2
0.5	68	$3.2 \cdot 10^{15}$	2-B2
1	68	$3.2 \cdot 10^{15}$	2-B2

EC50=68mg/L

Table S2. Concentration of graphene sheets was kept constant whilst drug concentration was systematically varied.

Graphene] g/L	[IBP] mg/L	Fe_3O_4 NPs/g Graphene	Figure
1	10	$3.2 \cdot 10^{15}$	2-A1
1	20	$3.2 \cdot 10^{15}$	2-A1
1	30	$3.2 \cdot 10^{15}$	2-A1
1	40	$3.2 \cdot 10^{15}$	2-A1
1	50	$3.2 \cdot 10^{15}$	2-A1
1	100	$3.2 \cdot 10^{15}$	2-A1

Graphene] g/L	[IDCF] mg/L	Fe3O4 NPs/g Graphene	Figure
1	10	$3.2 \cdot 10^{15}$	2-A2
1	20	$3.2 \cdot 10^{15}$	2-A2
1	30	$3.2 \cdot 10^{15}$	2-A2
1	40	$3.2 \cdot 10^{15}$	2-A2
1	50	$3.2 \cdot 10^{15}$	2-A2
1	68	$3.2 \cdot 10^{15}$	2-A2

Table S3. Concentration of concentration was kept constant while graphene systematically varied.

Graphene] g/L	[IBP] mg/L	Fe_3O_4 NPs/g Graphene	Figure
1	100	0	3-B
1	100	$3.2 \cdot 10^{14}$	3-B
1	100	$3.2 \cdot 10^{15}$	3-B
1	100	$3.2 \cdot 10^{16}$	3-B

Graphene] g/L	[IDCF] mg/L	Fe3O4 NPs/g Graphene	Figure
1	68	0	3-B
1	68	$3.2 \cdot 10^{14}$	3-B
1	68	$3.2 \cdot 10^{15}$	3-B

1	68	$3.2 \cdot 10^{16}$	3-B

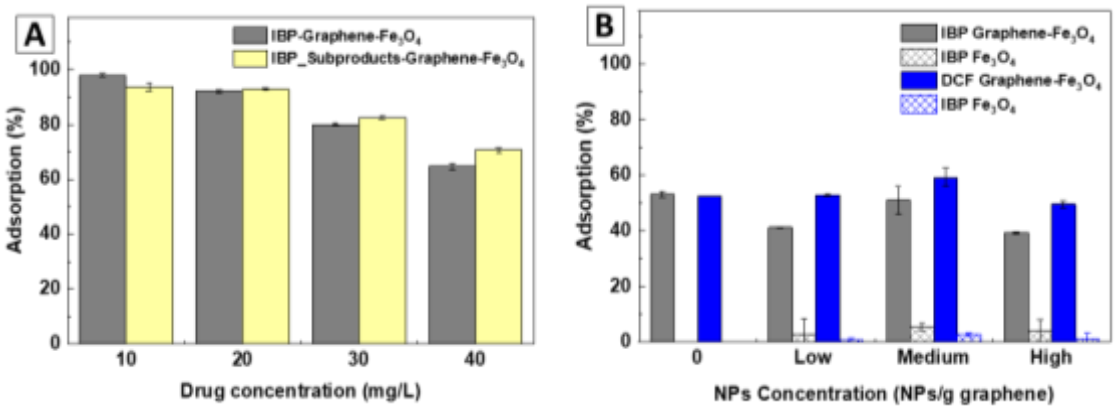

Figure S6. (A) Adsorption isotherms of Ibuprofen and Temporary byproducts in Graphene/Fe_3O_4/ hybrid nanostructures at different drug concentrations. (B) Drug adsorption onto the Graphene/Fe_3O_4/ hybrid nanostructures. loaded with different Fe_3O_4 concentration of NPs; low ($3.2 \cdot 10^{14}$ NPs/g graphene), medium ($3.2 \cdot 10^{15}$ NPs/g graphene), and high ($3.2 \cdot 10^{16}$ NPs/g graphene) when exposed to 100mg/L (grey) of IBP or 68mg/L DCF (blue). Controls of Fe_3O_4 NPs controls are represented in sparse patterns. Note that standard NP's concentration tested in Fig. 5. is $3.2 \cdot 10^{15}$ NPs/g graphene (medium)

The effect of Fe_3O_4 NPs on the adsorption performance of the hybrid was tested by studying drug degradation by NPs following site reactions. Comparing the UV-Vis signal of IBP (222 nm) and its temporary products (262 nm), it can be seen that signal ratio A(λ222nm)/A(λ =262nm) ≈ 25 during the complete exposition process. These results demonstrate that the adsorption of the drug as a whole entity. Otherwise, the degradation signal of the IBP feature would decrease while that of temporary products increase, indicating a Fenton-like reaction of the drug with the Fe_3O_4 NPs.